International Journal of Advances in Engineering and Management (IJAEM)
Volume 3, Issue 10 Oct 2021, pp: 521-535 www.ijaem.net ISSN: 2395-5252

Design, Construction and Performance Evaluation of A System for Assessing the Effect of Temperature and Humidity *On the Performance of A Pv Module

Ismaila Garba Saidu[1] and Aliyu Sulaiman Mindaudu[2]
[1]*Department of Physics, Usmanu Danfodio University Sokoto, Nigeria*
[2]*Department of Electrical Engineering, Umaru Ali Shinkafi Polytechnic, Sokoto*

Submitted: 01-10-2021 Revised: 10-10-2021 Accepted: 12-10-2021

ABSTRACT
The performance of photovoltaic modules when deployed in the field is affected by environmental factors. This study is designed to help provide a device that can be used to monitor the performance of a typical PV installation. The two weather parameters considered are temperature and humidity. Measuring instruments were designed to measure temperature, humidity, PV output current and voltage simultaneously. Provision was made to log the data at desired intervals. The logged data can be accessed wirelessly vie a Wi-Fi network. The devices constructed, when tested, were able to measure and log the intended parameters successfully at desired intervals. The accuracies of all the measuring devices when used to compare those measured by standard ones showed a very high degree of correlation with values greater than 90%. All the logged data could be accessed and downloaded remotely.

Keywords: PV, temperature, humidity, logging, efficiency

I. INTRODUCTION

Two problems associated with PV power generation have been the low energy conversion efficiency and the dependence of its performance on weather conditions (Zhou, 2016; Rahman, 2015). There are a number of factors, which affect PV output when operated in the field. These include intensity of solar radiation, air temperature, shading, wind speed and type of the material used to manufacture PV panels (Green et al., 2004; Schwingshackl et al., 2013; Peng (2017),Vasel and Iakovidis, 2017). Increase in temperature is said to affect negatively the output voltage whereas increase of irradiation increases the PV output current (Schwingshackl et al. (2013); Vasel and Iakovidis (2017) and Kaldellis et al. (2014)). Peng (2017) investigated the practical effects of solar PV surface temperature on output performance and reported that provision of cooling function on the back of solar PV panel increased efficiency of solar PV module almost by 47%. The voltage of a PV cell is highly dependent on its temperature and an increase in temperature decreases its voltage (Devabhaktuni et al, 2013). Figure 1 shows the effect of temperature on the I-V characteristic of a PV module at constant radiation (Qiang and Nan, 2010).

International Journal of Advances in Engineering and Management (IJAEM)
Volume 3, Issue 10 Oct 2021, pp: 521-535 www.ijaem.net ISSN: 2395-5252

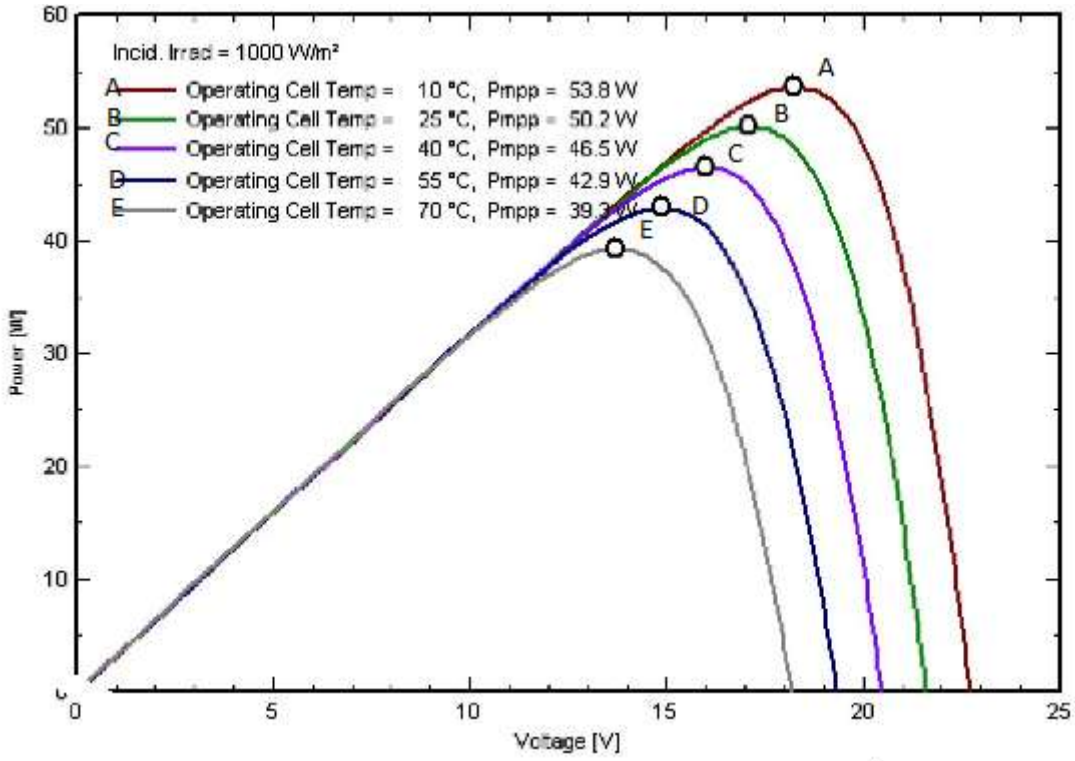

Figure 1: output P-V characteristics of the PV module with different temperatures (Fesharaki et al, 2011)

The implication of these is that hotter solar panels produce less energy from the same amount of sunlight. Relative humidity defined as the ratio of water vapour in the air to the maximum water vapour the air can hold at a given temperature. Various studies have shown that relative humidity has direct effect on the efficiency of a solar panel. In a study on the effect of humidity on PV performance, Kasem et al, (2012), used three types of solar photovoltaic; Monocrystalline, polycrystalline and amorphous silicon and found that relative humidity affects efficiency of photovoltaic as it affects the current, voltage and power. Their result showed that Monocrystalline panel has the highest efficiency when relative humidity is decreased with respect to other technologies. This is shown in Figure 2.

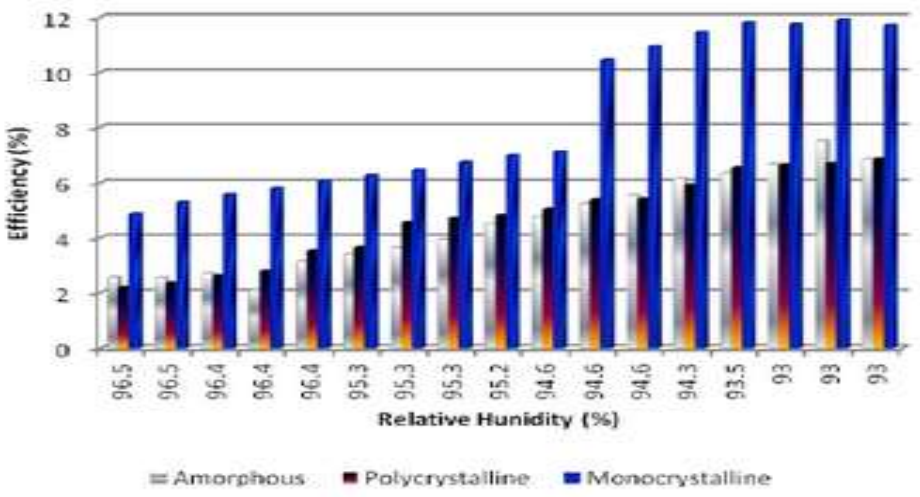

Figure 2: Relationship between humidity and efficiency for different technology (Kasem et al, 2012)

International Journal of Advances in Engineering and Management (IJAEM)
Volume 3, Issue 10 Oct 2021, pp: 521-535 www.ijaem.net ISSN: 2395-5252

Ettah et al, 2012 investigated in Calabar, Nigeria the effect of relative humidity on the performance of solar panels the results demonstrated that low relative humidity between 69% and 75% resulted in the increase in output current from solar panels. Omubo et al, 2009 using a B-K Precision modules 615 Digital light instrument and PV modules in Port Harcourt investigated the effect of relative humidity on the conversion of solar energy to electricity and found that there is a direct proportionality between solar flux, output current and efficiency of the PV module. The low relative humidity enhances the performance of solar panels (Ettah et al, 2012). In this paper, a device for assessing the effect of temperature and humidity on the performance of a PV installation is presented. The device is designed to measure and log the temperature and humidity around a deployed PV installation. Also included are provision for measuring and logging of the output current and voltage of a PV farm. The measured and logged current and voltage data can be used to evaluate the power of the PV. For ease of data harvest a provision is made for access to the data to be viewed or downloaded on a Wi-Fi network.

II. METHODOLOGY

2.1 Relative Humidity /Air Temperature Measurement Design and Construction

For the purpose of air temperature and humidity measurement, around the PV installation, an RHT-03 digital capacitive sensor was used. The RHT03 (also known as DHT-22) is a low cost humidity and temperature sensor with a single wire digital interface (Extech Instruments Corporation, 2008).

The RHT03 outputs a calibrated digital signal and sends data via a single wire line on request from the microcontroller. The sensor sends data at 5 byte per packet (Extech Instruments Corporation 20082) bytes for the temperature value 2 for humidity and the last byte for the bit check-sum. The data is comprised of integral and decimal part. The pins are numbered as shown from pin 1 to pin 4 (Figure 3).

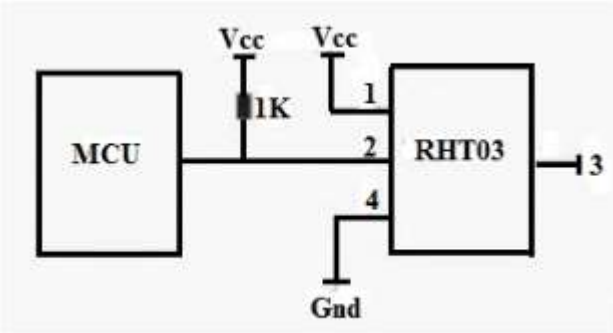

Figure 3: Circuit connection of RHT03 (Extech Instruments Corporation, 2008)

The pin configuration indicates that pin 1 serves as the positive power terminal (V_{DD}) while pin 4 is the ground (GND). As recommended by the data sheet of the chip, a 100nF capacitor was connected between the V_{DD} and ground to provide a low reactance part for the noise signal that could affect the accuracy of the sensor. Pin 2 serves as the devices bidirectional I/O terminal. The sensor uses a 1 wire bus as a dual directional digital data line cable of transmitting and receiving data over the same single wire. The pin was connected to pin 4 of port B of the microcontroller. As specified in the datasheet of the sensor a 1K resistor was connected to pull up pin 2 to the positive rail of the supply. Pin 3 was left unconnected as is normal with the chip. The circuit was constructed on a circuit board and tested (plate 1).

International Journal of Advances in Engineering and Management (IJAEM)
Volume 3, Issue 10 Oct 2021, pp: 521-535 www.ijaem.net ISSN: 2395-5252

Plate 1: Constructed circuit of the temperature and humidity unit

The circuit was then cased and protected from being exposed to a direct sunlight captured in plate 2 based on the recommendation from temperature and humidity sensor (Extech Instruments Corporation, 2008)

Plate 2: Temperature and relative humidity shield

2.2 **Current and Voltage Measurement**

To assess the performance of the PV installation at the prevailing temperature and humidity an ammeter and voltmeter based on the design by Saidu et al (2019) were constructed and incorporated to continuously measure and log the output currents and voltages of the PV plant. The ammeter circuit was realised using Hall Effect sensor shown in Figure 4 while the voltmeter is a potential divider attenuator shown in Figure 5.

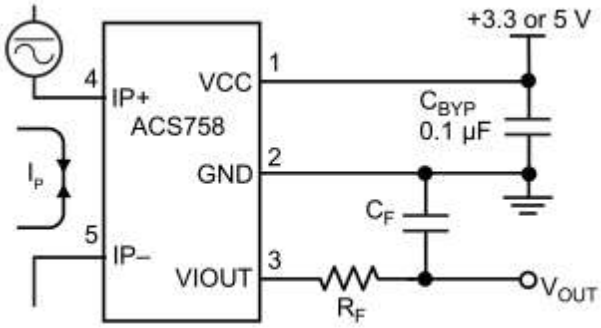

Figure 4: Hall Effect current sensor circuit (Saidu et al, 2019)

International Journal of Advances in Engineering and Management (IJAEM)
Volume 3, Issue 10 Oct 2021, pp: 521-535 www.ijaem.net ISSN: 2395-5252

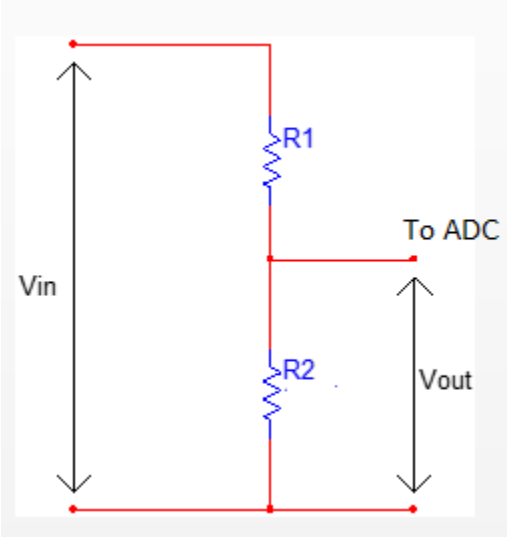

Figure 5: Potential divider attenuator (Saidu et al, 2019)

2.4 Microcontroller

The microcontroller effected the integration of the different system components and subsystems. The microcontroller was programmed to deliver dynamic HTML pages to web browser using the HTTP application-level protocol implemented by web servers. The pages were saved in the FLASH memory on the microcontroller and modified dynamically upon request by a front-end browser. The microcontroller was made to effect file creation and management tasks concerned with log archiving. A SLIP protocol implemented in the WIZ1000 Serial-To-Ethernet Converter enabled this embedded server to receive HTTP requests over the serial port, and return requested pages to the browser via same.

The embedded web server has the capability to download log files via the browser, delete log files, update system real time clock chip, and manage network connectivity, amongst others. Logs read from the attached SD card was formatted as HTML pages and presented to the browser for visualization.

Semi-permanent data storage was effected using an SD card. A FAT32 file system built on El Chan's FatFs open-source file system was implemented to handle file creation and management. The FatFs library was configured to meet just the basic functionalities required of the logger, such as short file names.

A real time clock chip (RTCC) was incorporated for a semi-permanent timekeeping. The RTCC was backed up by a 2.7v CMOS battery that sustained chip operation when the main system power is disconnected. The DS1307 RTCC sports an I2C interface, and was placed on the same bus as the 24C04 512-byte serial memory chip. The I2C port was emulated in software using bit-banging as it offered a more flexible approach to implementing various checks on the I2C bus. The RTCC initialization was effected via the browser on the PC-side of the user interface.

For unattended logger operation, certain parameters needed to be retained in non-volatile memory. These configurations were:

a. Log-in name
b. Log-in password
c. Logging interval
d. Network reset interval

These parameters were saved in a 512-byte serial EEPROM for recall during system operation.

The EEPROM enabled byte-programmability of the EEPROM array, unlike FLASH EEPROM where only sector-wide operations can be performed.

To interface the logger with an Ethernet network, an Ethernet interface needed to be integrated into the system. The Ethernet interface was required to provide serial-to-Ethernet conversion capability, enabling the microcontroller to received TCP-IP packets as binary data over the UART, and also send binary data over the UART to be encoded into Ethernet packets by the converter. A high-capability converter fitting this requirement was found in the WIZ1000.

The WIZ1000 is manufactured by WIZnet. The device acts as a gateway between RS232 and Ethernet. It enabled remote gauging, managing, and control of a device through the

International Journal of Advances in Engineering and Management (IJAEM)
Volume 3, Issue 10 Oct 2021, pp: 521-535 www.ijaem.net ISSN: 2395-5252

network based on Ethernet and TCP-IP by connecting to the existing equipment over RS232 serial interface. It is a protocol converter that transmits the data sent over the RS232 serial port to TCP-IP data packets, and converts TCP-IP data received over the Ethernet network into serial data that is sent out over the serial port. The WIZ1000 was configured with a static IP address since it was configured as a server, making it reachable over the network.

To emplace the logger on a wireless network an interface is required between the Ethernet port on the converter and the wireless network. A Mikrotik SX-5nD2 Consumer Premise Equipment/Router is configured as a bridge. The CPE bridges the LAN Ethernet on the WIZ1000 with any wireless network to which it is configured to connect with.

2.5.0 TESTS

2.5.1 Thermometer and Hygrometer Performance Test

To test for the performance of the temperature and humidity measuring devices a digital thermometer type (ST-9269 Multi-Stem Thermometer) and hygrometer were used to conduct an exercise to compare the measurements of the two sets of meters. A water jug was half-filled with water with blocks of ice-water dropped into the water to achieve low temperature. The two thermometers and hygrometers (reference and constructed) were hung just above the covered water to measure the temperature and humidity above the water. The temperature of the enclosure and humidity as recorded by the two thermometers and two hygrometers were measured at intervals and the results tabulated in Table 1 and Table 3 respectively. In order to get higher temperatures and humilities, a water heater was inserted into the water and switched on. As the temperature of the water rose, measurements were taken at different intervals by the two sets of meters. The measurements continued until the water boiled.

2.5.2 Performance Test of Ammeter

To assess the performance of the ammeter three cases were considered. The aim was to test for its accuracy in measuring low, medium and high currents.

Case 1A: In the first case a simple circuit shown in Figure 6 was implemented. The circuit was designed to measure currents in the microampere range. The fabricated meter and a reference standard digital meter (MIC-2200A) were used to measure the same currents for comparison. A1 is the constructed ammeter while A2 is a reference one.

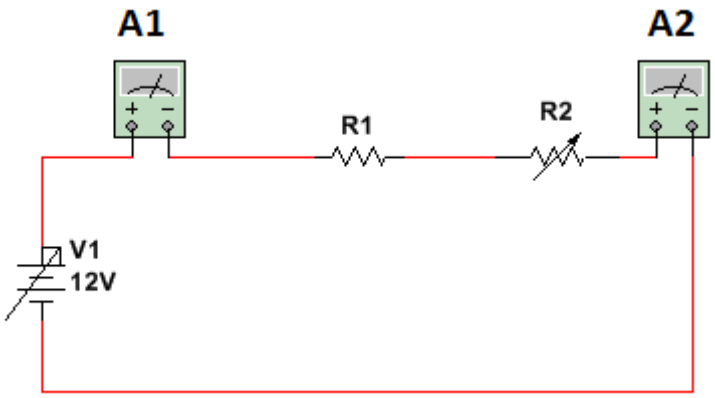

Figure 6: Set up to assess the performance of the fabricated ammeter in measuring low currents.

R1 is a 100 Ω, protective resistor, to prevent the battery from shunting. R2 is a variable resistor of value 1 MΩ. The variable resistor was varied to obtain different values while noting the values of A1 and A2 at each resistance value. The results obtained were plotted in Figure 11.

Case 2: R1 was then replaced with a 10 Ω, 5 Watts resistor, while R2 was replaced with a resistance decade box (J.J Lyod Instruments). The decade box was used to set different resistance values in order to vary the circuit current. The values, as measured by the two meters, were plotted in Figure12.

Case 3: To test for higher currents the meters were used to measure the output short circuit currents of a PV installation at the Sokoto State Polytechnic at different times of the day. Care was taken not to leave the standard meter connected for a long time as this could damage the meter due to the high

International Journal of Advances in Engineering and Management (IJAEM)
Volume 3, Issue 10 Oct 2021, pp: 521-535 www.ijaem.net ISSN: 2395-5252

currents from the PVs. The results obtained are plotted in Figure 13

2.5.3 Test of Voltmeter Performance

To test the performance test of the fabricated test the meter was used to compare a standard reference one. Two cases were considered to see how it could measure high and low voltages.

To achieve this, a simple circuit as shown in figure was implemented. Two voltmeters (Reference and fabricated) were connected as shown Figure 7.

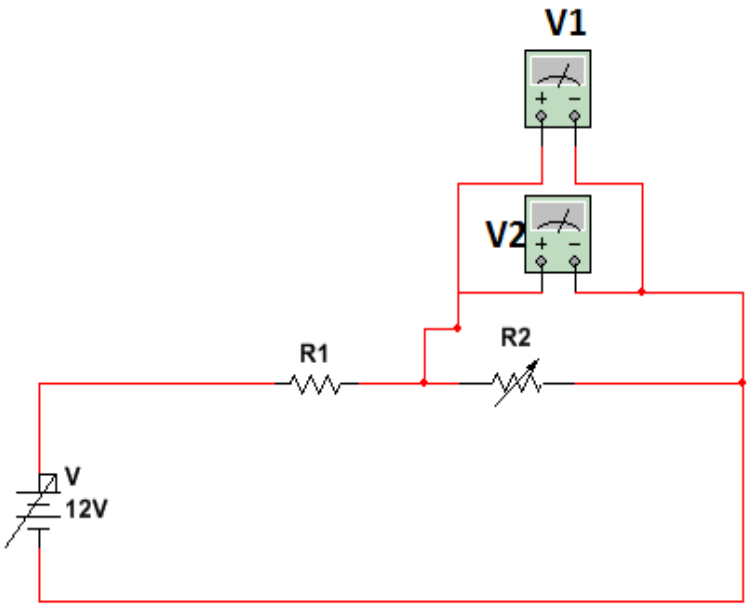

Figure 7: Voltage performance test circuit

Case 1: V1 (Standard digital voltmeter) and V2 (Fabricated Voltmeter) are connected in parallel to measure the voltages across R2 concurrently. R1 is a 100 Ohms 2 Watts resistor while R2 is a 10 K variable resistor. The variable resistor is varied gradually from left to right to obtain different voltages across the resistor R2 as recorded by the two voltmeters.

The values obtained were plotted in Figure 14

Case2: In order to measure higher values the two voltmeters were use to measure the output open circuit voltages of a combination of solar modules placed in the open.

The modules were connected in series and the voltages measured as shown at the points marked A, B, C, D, and E (Figure 8). The result obtained was plotted in Figure 15

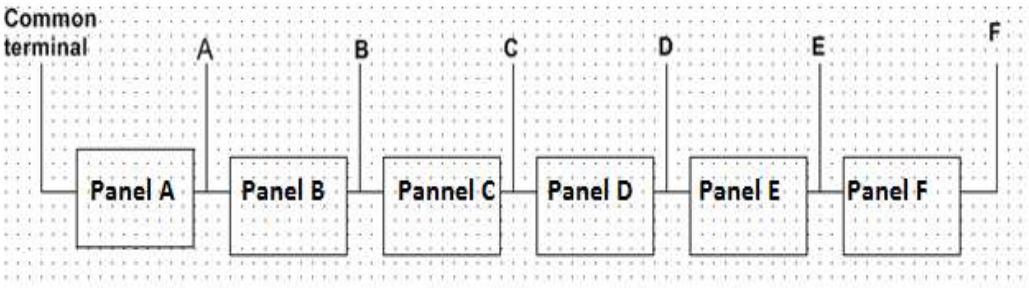

Figure 8: Performance test of voltmeter at high voltages

2.5.4 System Field Assessments

The system was then placed in the open to log weather data. The power required by the assembly was provided by using two lithium ion batteries a charger and solar panels. Under test the two batteries could provide supply to the system for thirty seven hours when fully charged. The

International Journal of Advances in Engineering and Management (IJAEM)
Volume 3, Issue 10 Oct 2021, pp: 521-535 www.ijaem.net ISSN: 2395-5252

system's logger was accessed through a server and a Wi-Fi radio from a laptop computer.

III. RESULTS

3.1 Result of the Performance Test of the Fabricated Thermometer

The result obtained in the evaluation of the performance of the constructed thermometer was tabulated and the percentage error evaluated using the formula:

Percentage error Pt = $\frac{[\sum Tr - Tf]}{\sum Tr}$ x 100

= 4.5%

Where Tr is the temperature of reference

Tf is the temperature of the fabricated

To evaluate the fabricated thermometer characteristics the result was plotted in Figure 9

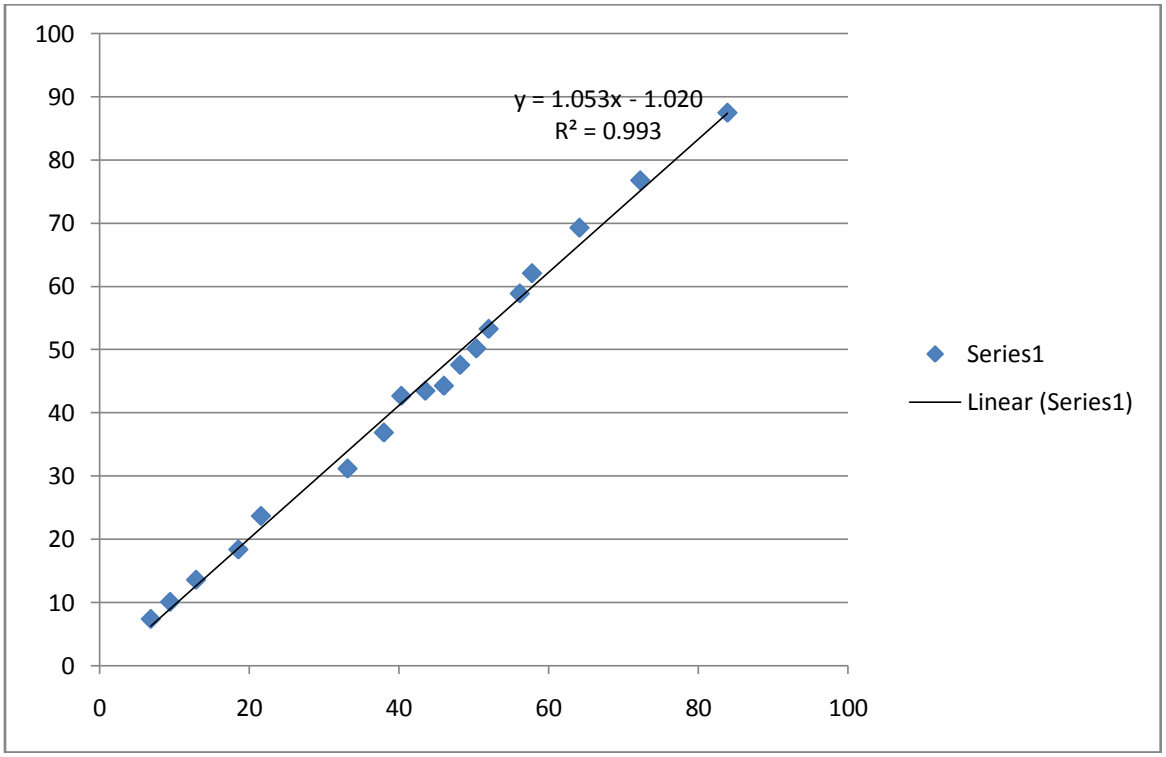

Figure 9: A plot of the performance of the Thermometer

The characteristics of the fabricated thermometer is summarized in Table 1

Table 1: Summary of the characteristics of the fabricated thermometer

Characteristics	Value
Linearity	99.3%
Sensitivity	1.053
Range	-45°C to 125°C
Percentage error	4.5%
Transfer function	y = 1.053x - 1.020
R^2	R² = 0.993

3.2. Result of the Performance Test on the Fabricated Hygrometer

The result of the test to relate the measurements of the constructed hygrometer (Hf) when compare to that of a reference hygrometer (Hr) is plotted in Figure 10

And the percentage error was evaluated Percentage error Ph = $A_e = \frac{[\sum Hr - Hf]}{\sum Hr}$ x 100

= 8.05%

International Journal of Advances in Engineering and Management (IJAEM)
Volume 3, Issue 10 Oct 2021, pp: 521-535 www.ijaem.net ISSN: 2395-5252

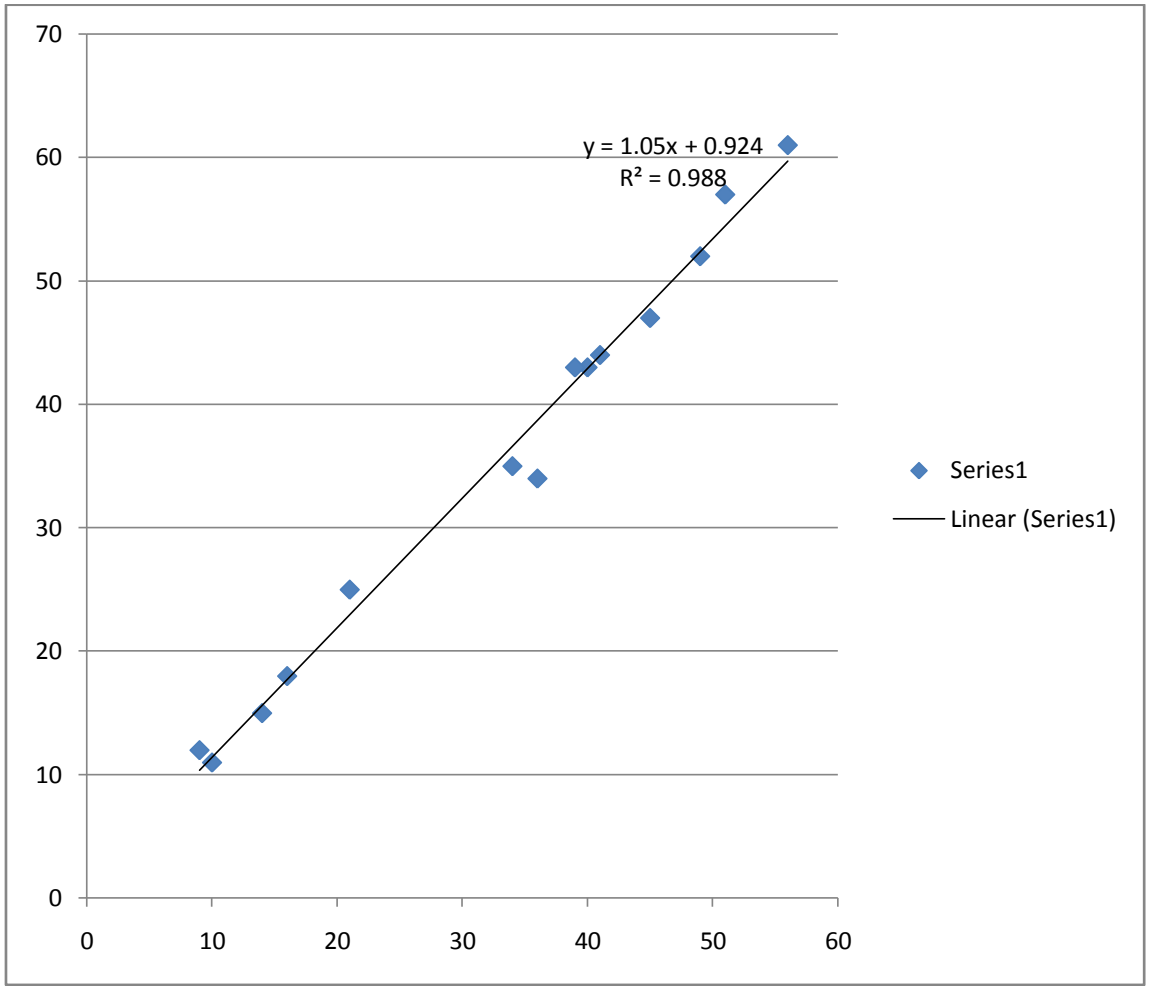

Figure 10: Graph of the performance of hygrometer

The results of the hygrometer test is summarised in Table 2.

Table 2: Summary of the characteristics of hygrometer

	Characteristics	Value
1	Linearity (R^2)	0.998
2	Sensitivity	1.05
3	Range	0-100%
4	Percentage error	8.05%
5	Transfer function	y = 1.05x + 0.924

3.3 Result of the Ammeter Performance Test

The ammeter performance assessment was conducted in three parts: low current values, medium current value and high current values.

Case one: The result obtained in the test to compare the fabricated ammeter and a standard one, for low current values, was plotted using the MINITAB software in Figure 10. A scatter plot was first plotted then fitted with a line of best fit which is linear. The test was mainly to see how the meter would perform when used to measure currents in the microampere range.

International Journal of Advances in Engineering and Management (IJAEM)
Volume 3, Issue 10 Oct 2021, pp: 521-535 www.ijaem.net ISSN: 2395-5252

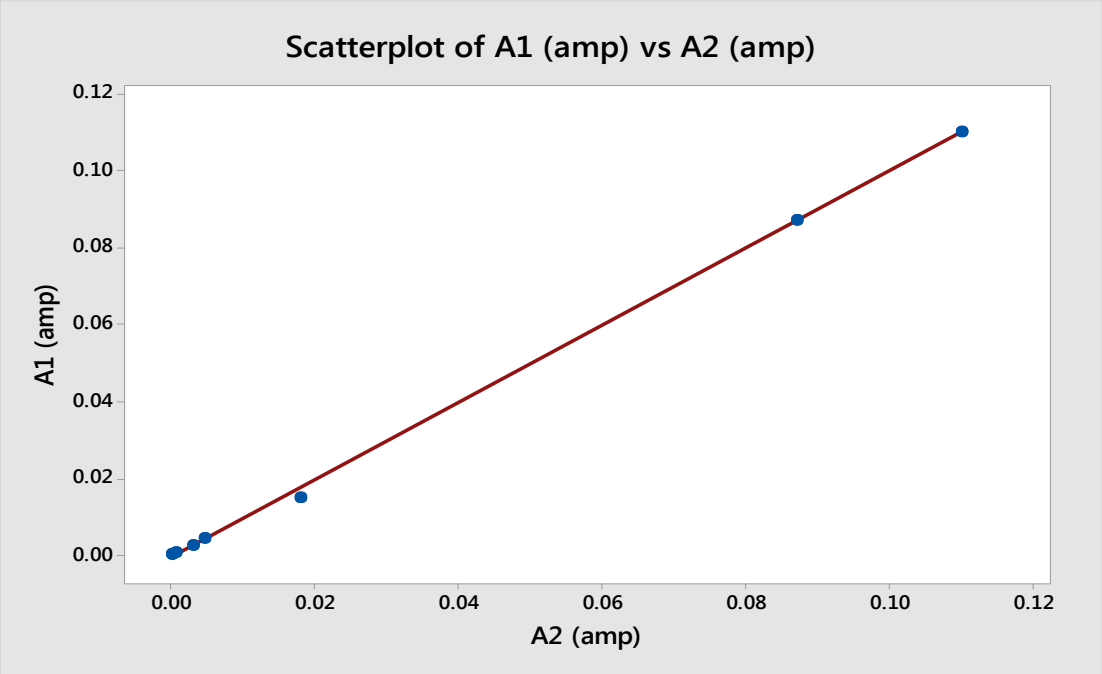

Figure 11: A plot of a graph to test for the ability of the fabricated ammeter to measure current in the microampere range.

The Pearson correlation coefficient (R^2) was 0.999 while the transfer function is y = 0.995x
This value indicates that the line of intercept is zero while the sensitivity at this lower range of the device is 99%.

Case Two: The result obtained from the test on the performance of the constructed ammeter on medium value currents is plotted in Figure 11. The MINITAB software plot is fitted with a linear line as shown.

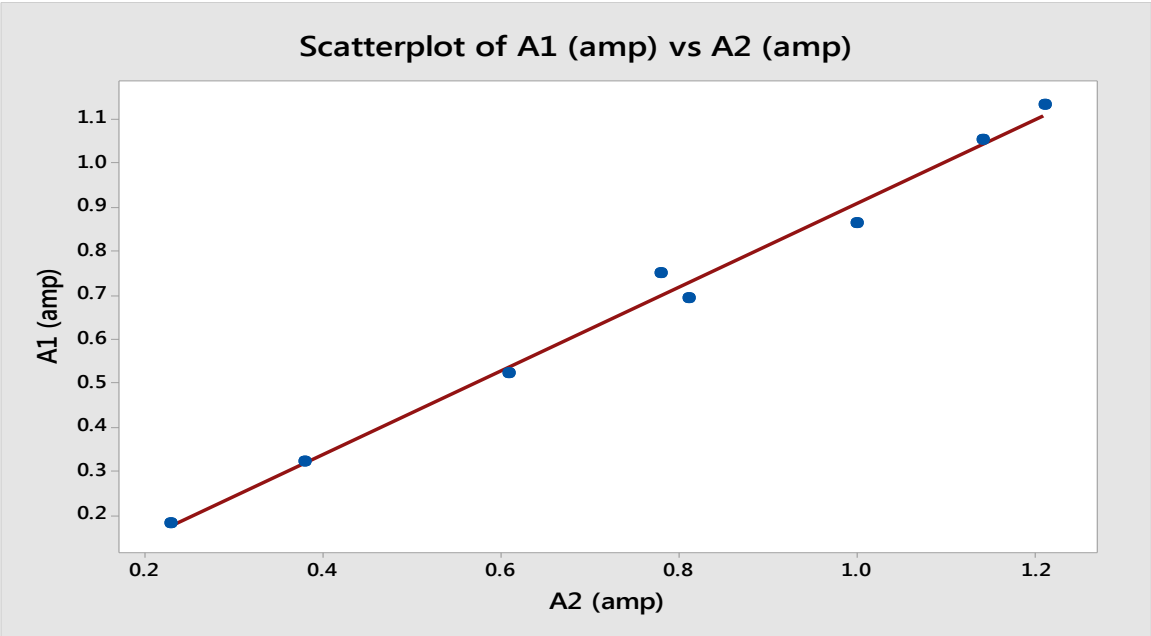

Figure 12: A plot of the ammeter test on its ability to measure medium value currents

International Journal of Advances in Engineering and Management (IJAEM)
Volume 3, Issue 10 Oct 2021, pp: 521-535 www.ijaem.net ISSN: 2395-5252

The equation relating the two quantities was also shown to be:
y = 1.040x + 0.054

Where Y is the result of the fabricated meter and x is that of the reference meter. The correlation coefficient value was 99%.

Case Three: The last test conducted was to ascertain the capability of the ammeter to measure relatively high currents. The result obtained is plotted in Figure 12

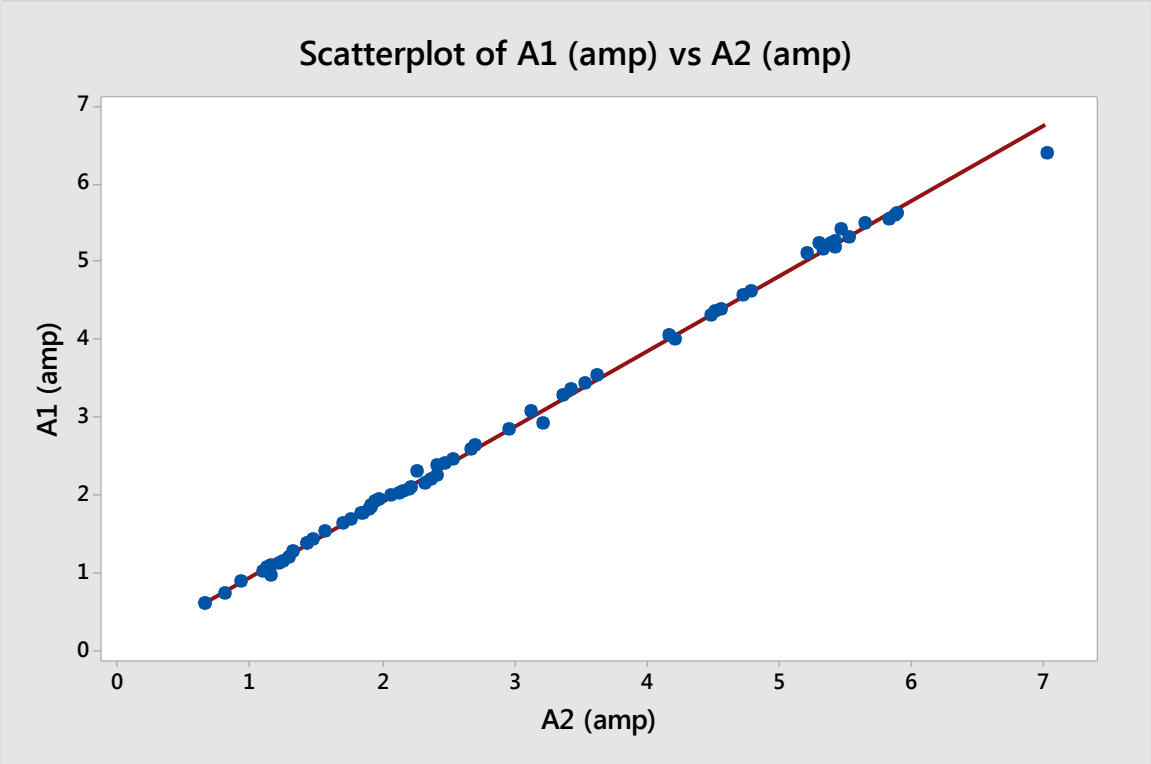

Figure 13: The plot of the result obtained from the test on high value currents.

The transfer function relating the two meters (reference [X] and fabricated [y]) is
y = 1.080x + 0.007
While the R^2 value is 0.957

3.4 Result of the Performance Test on the constructed Voltmeter

To test the performance of the constructed voltmeter, two tests were conducted. The first test was for low voltages while the second one was on higher voltages.

Case One: The result obtained during the test to ascertain the performance of the voltmeter in measuring low voltages is used to plot the graph of Figure 13. ,

International Journal of Advances in Engineering and Management (IJAEM)
Volume 3, Issue 10 Oct 2021, pp: 521-535 www.ijaem.net ISSN: 2395-5252

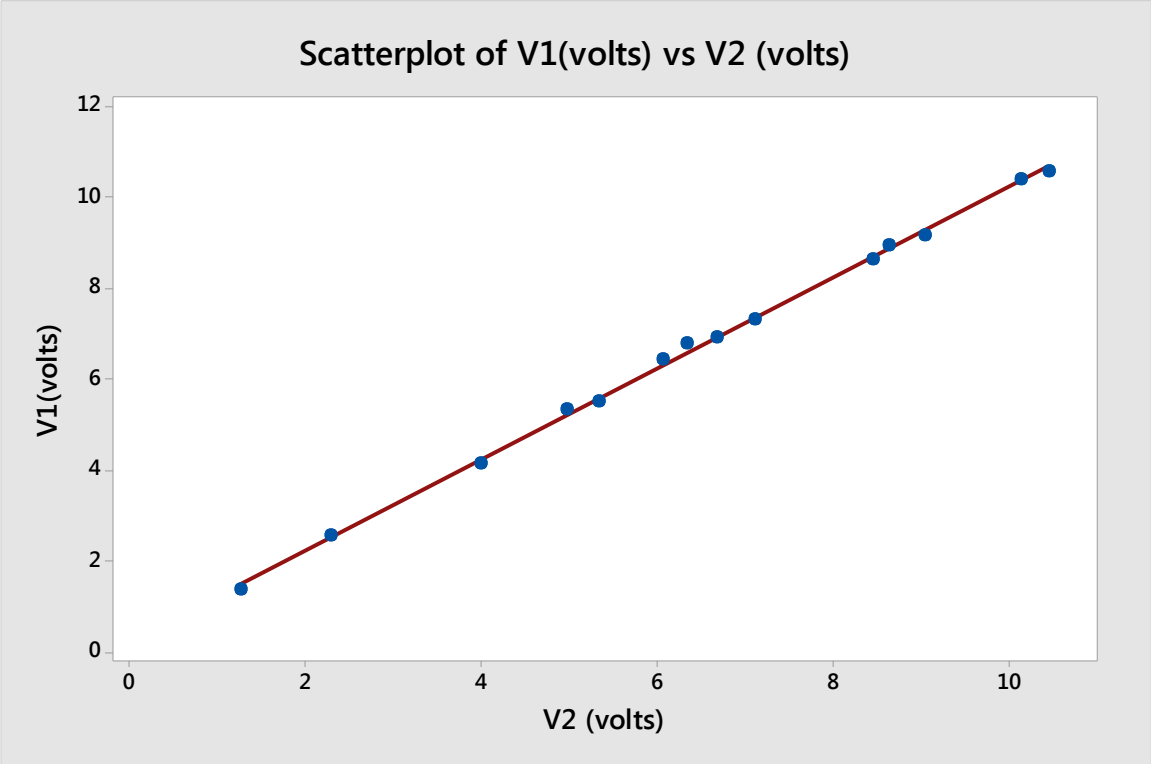

Figure 14: The result of the performance test on measuring low voltages

The transfer function relating the two meters (constructed and standard) is y = 0.960x - 0.07 while the R^2 value is 0.997. The sensitivity is 96%.

Case Two: The result of the test on the performance of the constructed voltmeter in measuring high voltages is plotted in Figure 14.

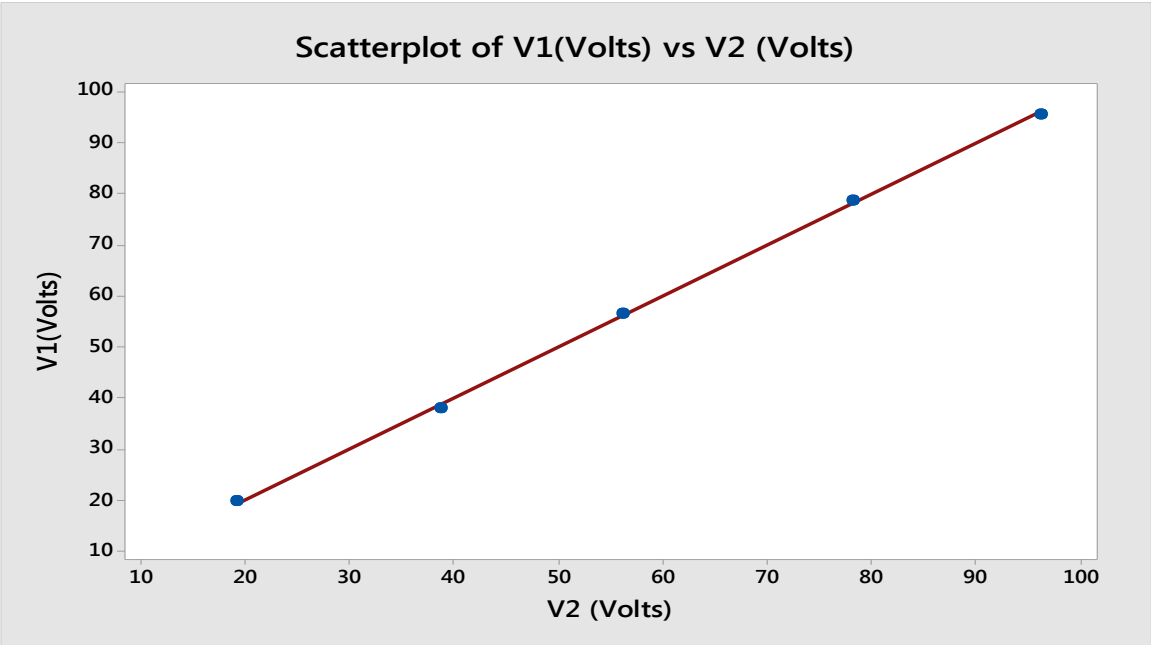

Figure 15: The performance test of the voltmeter at high voltages.

International Journal of Advances in Engineering and Management (IJAEM)
Volume 3, Issue 10 Oct 2021, pp: 521-535 www.ijaem.net ISSN: 2395-5252

The transfer function of relating the two meters is: $y = 1.002x - 0.198$. The R^2 value is 0.99.

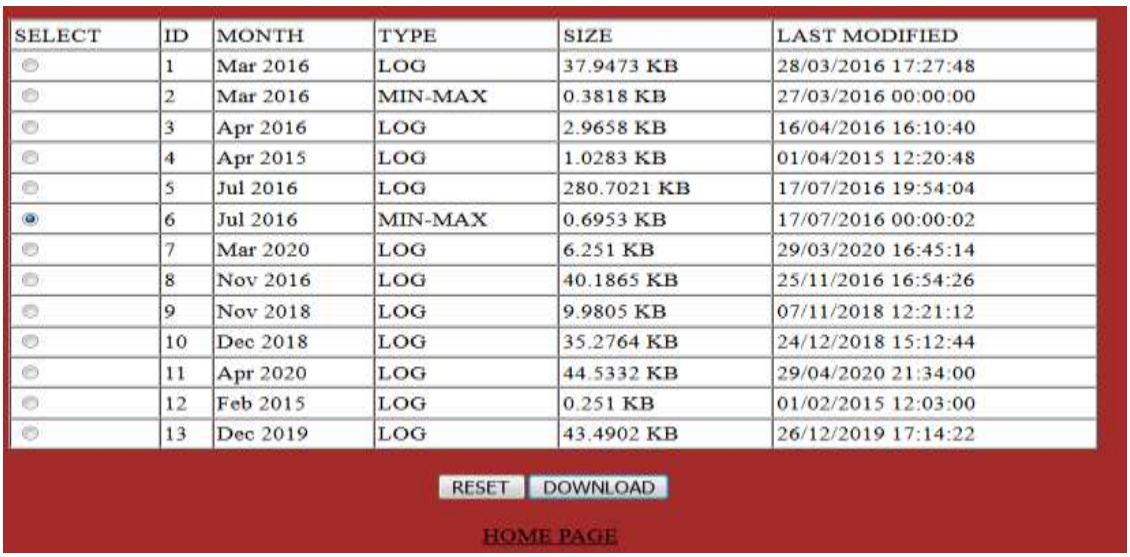

SELECT	ID	MONTH	TYPE	SIZE	LAST MODIFIED
○	1	Mar 2016	LOG	37.9473 KB	28/03/2016 17:27:48
○	2	Mar 2016	MIN-MAX	0.3818 KB	27/03/2016 00:00:00
○	3	Apr 2016	LOG	2.9658 KB	16/04/2016 16:10:40
○	4	Apr 2015	LOG	1.0283 KB	01/04/2015 12:20:48
○	5	Jul 2016	LOG	280.7021 KB	17/07/2016 19:54:04
◉	6	Jul 2016	MIN-MAX	0.6953 KB	17/07/2016 00:00:02
○	7	Mar 2020	LOG	6.251 KB	29/03/2020 16:45:14
○	8	Nov 2016	LOG	40.1865 KB	25/11/2016 16:54:26
○	9	Nov 2018	LOG	9.9805 KB	07/11/2018 12:21:12
○	10	Dec 2018	LOG	35.2764 KB	24/12/2018 15:12:44
○	11	Apr 2020	LOG	44.5332 KB	29/04/2020 21:34:00
○	12	Feb 2015	LOG	0.251 KB	01/02/2015 12:03:00
○	13	Dec 2019	LOG	43.4902 KB	26/12/2019 17:14:22

Plate 3: Screenshot of the server logs page.

This page allows the reset of the logs, delete a particular log or all the logs on the SD card and finally the logged data can be downloaded from this page. To do any of these the month or type of data that is desired to be operated on is first selected by checking or marking the circle under the select column. It is worth noting that provision is also made for the raw historic logs or the minimum and maximum daily logs to be downloaded. A particular period was selected and downloaded shown in Table 3.

Table 3: Potion of the logged data

DATE	TIME(UTC)	VOLTAGE(V)	CURRENT(A)	AIR HUM (%)	AIR TEMP (CELSIUS)
4/6/2021	12:37:57	18.54	4.42	22	32.4
4/6/2021	12:38:57	18.56	4.33	23	31.6
4/6/2021	12:39:57	18.54	4.35	23	31.35
4/6/2021	12:40:58	18.54	4.47	23	32.43
4/6/2021	12:41:58	18.65	4.32	23	32.43
4/6/2021	12:42:58	18.65	4.27	21	31.35
4/6/2021	12:43:58	18.48	4.32	23	31.35
4/6/2021	12:44:58	18.37	4.42	23	32.43
4/6/2021	12:45:58	18.56	4.32	23	32.43
4/6/2021	12:46:58	18.45	4.33	21	31.35
4/6/2021	12:47:58	18.67	4.33	22	31.78
4/6/2021	12:48:58	18.68	4.61	22	31.54
4/6/2021	12:49:58	18.48	4.35	23	31.35
4/6/2021	12:50:58	18.71	4.28	23	32.43
4/6/2021	12:51:58	18.35	4.51	23	32.43
4/6/2021	12:52:58	18.39	4.23	23	31.35
4/6/2021	12:53:58	18.72	4.5	23	31.35
4/6/2021	12:54:58	18.38	4.34	23	32.43
4/6/2021	12:55:58	18.38	4.51	23	31.35

International Journal of Advances in Engineering and Management (IJAEM)
Volume 3, Issue 10 Oct 2021, pp: 521-535 www.ijaem.net ISSN: 2395-5252

IV. DISCUSSION

Both the graphs comparing the measurements of the humidity and temperature to those measured by standard reference meters showed very good correlation with coefficient of over 90% for temperature and humidity. The errors of 4.5% for temperature and 8.5% for humidity was also not too much. The range of the sensor used indicates that the temperature range measurerable by the DHT sensor is -40^0C to 125^0C (Extec instrument Coporation, 2008) while the fabricated hygrometer has a range of 0% to 100%. These ranges are adequate for the intended application

The first test for the ammeter which was to determine the suitability of the meter in measuring low currents showed that the ammeter is capable of measuring accurately current with the milliampere range. There was a good correlation with almost unity coefficient between the measurement by the ammeters (constructed and reference (MP3100A). The transfer function relating the two meters was y= 0.99x+000. The constant value in the equation is zero showing that the meter does not have a zero error. The implication of this is that there may not be need for applying a negative or positive bias voltage for the measuring unit. The result of the second ammeter test and that of ampere range showed high accuracy with correlation of almost unity. The sensitivity of the meter which is represented by the slope of the graph (Fraden, 2003) is almost unity.

The datasheet of the Hall Effect sensor used could measure hundreds of amperes (Allegro Micro Systems, 2014). When measuring high currents in say hundreds of amperes care must be taken to use a much thicker cable capable of handling the high current. The high current however does not pose any danger to the ammeter itself as it is completely isolated from the current being measured.

The voltage measurement test outcome as plotted indicates a nearly perfect relationship between the fabricated and reference voltmeter. The R^2 value of over 0.90 is good enough for the targeted application. The voltmeter is capable of measuring voltages of up to 100 V.

A PC or android phones could be used to communicate with the systems if located within the WI-FI network of its server. The server was able to successfully upload results on a client's request. The ADM page's security when tested was found to be secured as only the administrator with the correct password could access the page. This ensures that the data in the logger is secured and protected from corruption or tempering. It ensures that the client has access only to view instantaneous data or download historical data saved on the SD card of the logger. This feature of the server enables the administrator detect from his PC if any part of the logger such as the RTC, the EEPROM is functioning well. This is very necessary as they affect the validity of the data logged. The flexibility of the Logger GUI application allows for data management through querying by one or more fields. A client or a number of clients could download data from the logger SD card saved with ".CSV" (comma-separated values) file extension. The retrieved data can be analysed using packages such as Microsoft Excel, Matlab, or SPSS.

V. CONCLUSION

In this paper we have been able to develop a system for logging the temperature and humidity data around a PV farm. These parameters have been identified by researches to have effect on the performance of PV module. To assess the output performance of the PV farm the electrical characteristics record of the current and voltages of the PV is logged. To achieve all these, measuring instruments were designed and their performances assessed. The performance evaluation of the instruments designed showed that their measurements are relatively accurate when compared to measurements of standard reference instruments. The output span of all the instruments shows that all the measuring devices could accommodate the intended range of measurement. The logging device was also able to log, successfully, all the parameters considered. The instantaneous and graphical values of the logged data were successfully viewed from a remote computer. The logged data was also available to clients on request.

REFERENCES

[1]. Allegro MicroSystems (2014). Thermally Enhanced, Fully Integrated, Hall Effect-Based Linear Current Sensor IC Allegro MicroSystems, Massachusetts U.S.A. www.allegromicro.com

[2]. Devabhaktuni V., Mansoor A., Soma S., Sreenadh R., Robert C. G, Douglas N. B., and Craig N. (2013) Renewable and

Sustainable Energy Reviews 19. (2013). Solar energy: Trends and enabling technologies journal homepage: www.elsevier.com/locate/rser

[3]. Extech Instruments Corporation, (2008). RHT03 data sheet.

[4]. http://www.alldatasheet.com/datasheet-pdf/pdf/295050/EXTECH/RHT10.html

[5]. Ettah E. B, Udoimuk A. B, Obiefuna J. N., and Opara F. E., "The Effect of Relative Humidity on the Efficiency of Solar Panels in Calabar, Nigeria", Universal Journal of Management and Social Sciences, Vol. 2, No. 3, March 2012, pp. 8-11.

[6]. Fesharaki V.J., Dehghani M., Fesharaki J. J., and Hamed T. (2011) The Effect of Temperature on Photovoltaic Cell Efficiency Proceedings of the 1st International Conference on Emerging Trends in Energy Conservation - ETEC Tehran, Tehran, Iran, 20-21 November 2011

[7]. Fraden, J. (2003) Handbook of Modern Sensors Physics, Designs, and Applications T h i r d E d i t i o n JACOB FRADEN Advanced Monitors Corporation AIP Press San Diego, California

[8]. Green MA, Basore PA, Chang N, Clugston D, Egan R, Evans R, Hogg D, JarnasonS, Keevers M, Lasswell P, Sullivan JO, Schubert U, Turner A,WenhamSR, YoungT. (2004) Crystalline silicon on glass (CSG) thin-film solar cell modules. Solar Energy77:857–63.

[9]. Kaldellis J. K,Marina K. , Kosmas A and. Kavadias (2014). Need for measurement of evaluation of the performance of pv installations on deployement.Renewable Energyhttps://doi.org/10.1016/j.renene.2013.12.041Volume 66, June 2014, Pages 612-62

[10]. Kasem H. A,.Aljibori H. S,.Hasoon F. N and. Chaichan M. T, (2012) Design and testing of solar water heaters with its calculation of energy, International.Journal.ofMechanical Computational and Manufacturing Research, vol. 1. No.2, / 62-66,

[11]. Saidu I. G., Momoh M. Moreh A. U. and Yahaya H. N. (2019). Design and Implementation of a Device for the Determination of the Effect of Soiling on Photovoltaic Panel Performance. Caliphate Journal of Science and Technology. /44-52

[12]. Schwingshackl C, Petitta M, Jochen E. Wagner J, E, Belluardo G, Moser D.C, Castelli M, Zebisch M, Tetzlaff A. (2013)Wind effect on PV module temperature: Analysis of different techniques for an accurate estimation Energy Conversion and ManagementDOI:10.1016/j.egypro.2013.08.010 455–461

[13]. Vasel A, FrantzisIakovidis F (2017) The effect of wind direction on the performance of solar PV plants Energy Conversion and Management: Elsevier. 1 December 2017 © 2017 Elsevier Ltd. All rights reserved. 455-461

[14]. Omubo P, V.B, Israel-Cookey, C, and Alaminokuma, G.I., (2009) Effects of Temperature, SolarFlux and Relative Humidity on the Efficient Conversion of Solar Energy to Electricity. European Journal of Scientific Research, Vol. 35, No. 2, pp. 173-180.

[15]. Peng Z. (2017). Cooled solar PV panels for output energy efficiency optimization Energy Conversion Management http://dxdoiorg/101016/jenconman201707007

[16]. Qiang F. and Nan.T. (2010). A Complex-Method-Based PSO Algorithm for the Maximum Power Point Tracking in Photovoltaic System, in Information Technology and Computer Science (ITCS), Second Int Conference on, pp. 134-137.

[17]. Rahman M M (2015) Effects of various parameters on PV-module power and efficiency. Energy Conversion and Management 103 348-358

[18]. WIZnet (2012) Serial-To-Ethernet Converter module" WIZ1000 manual.

[19]. Zhou J. C (2016) Temperature distribution and back sheet role of polycrystalline silicon photovoltaic modulesApplThermEnghttp://dxdoiorg/101016/japplthermaleng201610095